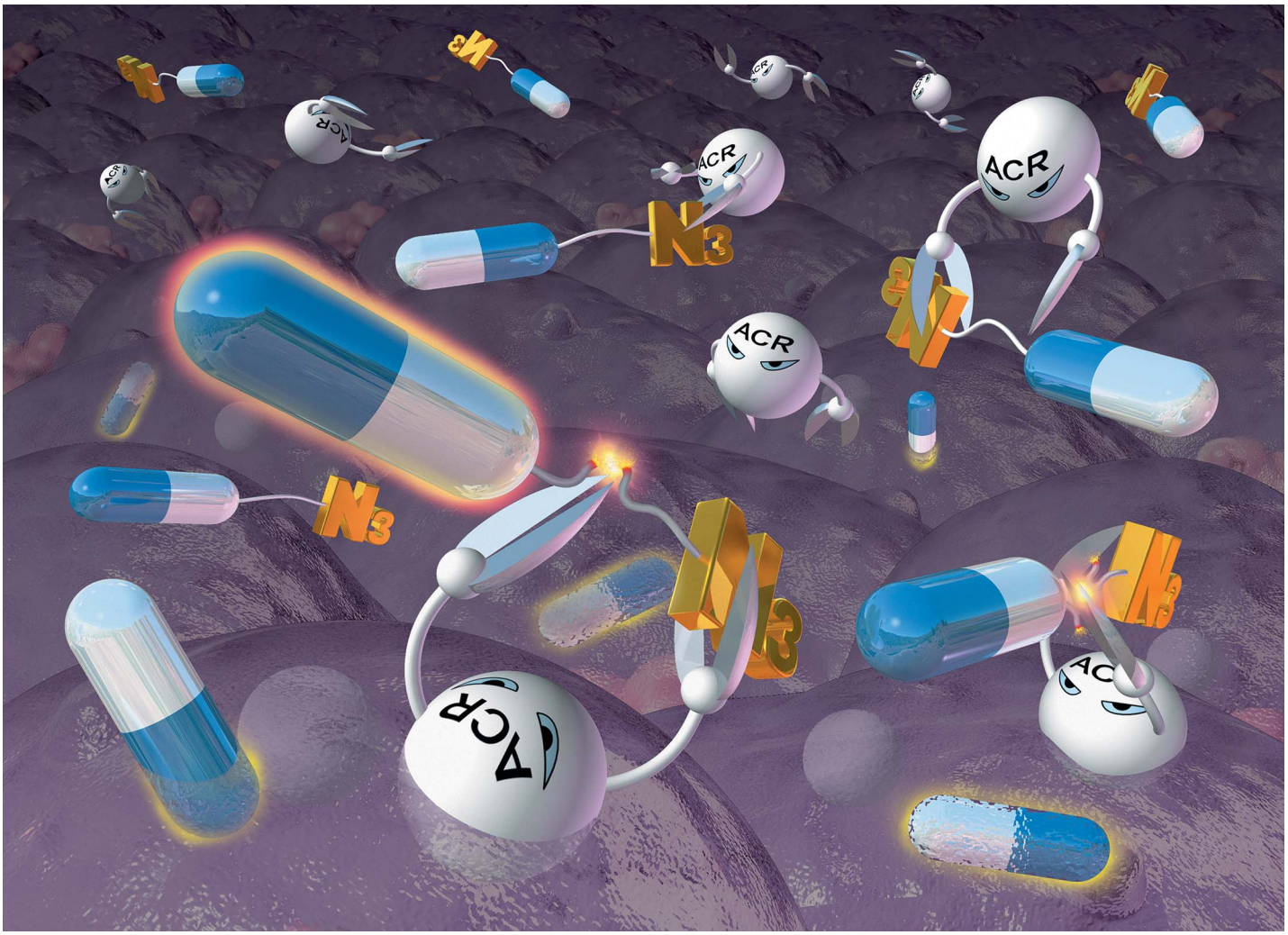

Showcasing research from Professor Katsunori Tanaka's laboratory, Tokyo Institute of Technology & RIKEN, Japan.

Targeted 1,3-dipolar cycloaddition with acrolein for cancer prodrug activation

An acrolein-targeted prodrug activation strategy was developed. Upon increasing the reactivity of azide on the experimental and theoretical basis, the endogenous acrolein on cancerous tissues efficiently reacted with prodrug through the azide-acrolein 1,3-dipolar cycloaddition to induce drug release only at the desired target area. Since acrolein is generally overproduced by most cancer cells and that was proved clinically in cancer patients by these authors, this research is anticipated as a starting point for clinical treatment with various cancers. Cancer drugs that have had selectivity challenges might be reconsidered for application by utilizing this strategy, i.e., "therapeutic in vivo synthetic chemistry".

As featured in:

See Ambara R. Pradipta, Katsunori Tanaka *et al.*, *Chem. Sci.*, 2021, **12**, 5438.

ROYAL SOCIETY OF CHEMISTRY

rsc.li/chemical-science

Registered charity number: 207890

Chemical Science

ROYAL SOCIETY OF CHEMISTRY

EDGE ARTICLE

View Article Online
View Journal | View Issue

Cite this: *Chem. Sci.*, 2021, **12**, 5438

All publication charges for this article have been paid for by the Royal Society of Chemistry

Received 4th November 2020
Accepted 16th March 2021

DOI: 10.1039/d0sc06083f

rsc.li/chemical-science

Targeted 1,3-dipolar cycloaddition with acrolein for cancer prodrug activation†

Ambara R. Pradipta, *[ab] Peni Ahmadi,[b] Kazuki Terashima,[a] Kyohei Muguruma,[a] Motoko Fujii,[a] Tomoya Ichino,[cd] Satoshi Maeda [cd] and Katsunori Tanaka *[abe]

Cytotoxic anticancer drugs used in chemotherapy are often antiproliferative agents that preferentially kill rapidly growing cancer cells. Their mechanism relies mainly on the enhanced proliferation rate of cancer cells and is not genuinely selective for cancer cells. Therefore, these drugs can also significantly affect healthy cells. Prodrug therapy provides an alternative approach using a less cytotoxic form of anticancer drug. It involves the synthesis of inactive drug derivatives which are converted to an active form inside the body and, preferably, only at the site of cancerous tissues, thereby reducing adverse drug reaction (ADR) events. Herein, we demonstrate a prodrug activation strategy by utilizing the reaction between aryl azide and endogenous acrolein. Since acrolein is generally overproduced by most cancer cells, we anticipate our strategy as a starting point for further applications in mouse models with various cancers. Furthermore, cancer drugs that have had therapeutic index challenges might be reconsidered for application by utilizing our strategy.

Introduction

Adverse drug reactions (ADRs) are the decisive risk factor associated with cancer chemotherapy, leading to toxic side effects and poor efficacy.[1] In general, to reduce ADRs, monoclonal antibody-directed enzyme therapy has been used in the targeted delivery of prodrugs to cancer cells.[2] Alternatively, one could activate a systemic prodrug *via* a change in the pH environment of the cancerous tumor.[3–5] In this case, the changes are often so modest that the selective activation of prodrug molecules is low, with the linkers susceptible to non-specific off-target hydrolysis. Another appealing alternative is the targeting of tumors through endocytosis of polymer–drug conjugates, followed by drug release.[6–8] However, this approach could be inherently slow and lacks direct temporal and quantitative control over drug release.

In the past decade, bioorthogonal chemistry has found broad applications, including prodrug activation strategies.[9] For example, although no biological data was presented, Florent and co-workers described the initial proof of concept on the utilization of Staudinger ligation followed by a self-immolation reaction to release doxorubicin from its prodrug (ESI, Fig. S1†).[10] Alternatively, Robillard and co-workers showed that the transformation of an azide to an amine group by a Staudinger reaction could be used to trigger drug release.[11] Gamble and co-workers utilized *trans*-cyclooctene-azide cycloaddition to mitigate the limitations associated with phosphine reagents used for prodrug activation.[12] Meanwhile, Robillard and co-workers demonstrated a drug release strategy by utilizing an inverse electron-demand Diels–Alder reaction between *trans*-cyclooctene and tetrazine cycloaddition.[13] More recently, activation of a systemic prodrug *via* cleavage of a deactivating linker on the prodrug triggered by an overexpressed enzyme or localized activation agent on cancer cells has been reported.[14–16] Nonetheless, in most cases, the enzyme is not naturally overexpressed at the cancer site, and enrichment or genetic modification is required to accumulate the activation agent. Despite this progress, co-administration of a prodrug with other exogenous activating agents could significantly induce immunogenicity and might hamper repeated administration.

Inspired by the initial bioorthogonal reaction strategies and the remaining *in vivo* application challenges, we set out to utilize a bioorthogonal prodrug activation reaction based on the 1,3-dipolar cycloaddition between endogenous acrolein and aryl azide. Acrolein, the most reactive α,β-unsaturated aldehyde,[17] has long been known to be a critical biomarker associated with various types of disorders related to oxidative stress, including

[a]*Department of Chemical Science and Engineering, School of Materials and Chemical Technology, Tokyo Institute of Technology, 2-12-1 Ookayama, Meguro, 152-8552, Tokyo, Japan. E-mail: pradipta.a.aa@m.titech.ac.jp; tanaka.k.dg@m.titech.ac.jp*

[b]*Biofunctional Synthetic Chemistry Laboratory, Cluster for Pioneering Research, RIKEN, 2-1 Hirosawa, Wako, 351-1098, Saitama, Japan*

[c]*Department of Chemistry, Faculty of Science, Hokkaido University, Kita 10 Nishi 8, Kita, 060-0815, Sapporo, Japan*

[d]*Institute for Chemical Reaction Design and Discovery (WPI-ICReDD), Hokkaido University, Kita 21 Nishi 10, Kita, 001-0021, Sapporo, Japan*

[e]*Biofunctional Chemistry Laboratory, Alexander Butlerov Institute of Chemistry, Kazan Federal University, 18 Kremlyovskaya Street, 420008, Kazan, Russian Federation*

† Electronic supplementary information (ESI) available. See DOI: 10.1039/d0sc06083f

cancer and Alzheimer's disease.[18] Acrolein is produced through the enzymatic oxidation of polyamines and is also generated during reactive oxygen species (ROS)-mediated oxidation of highly unsaturated lipids.[19–21] It is sometimes generated on μM scales in oxidatively stressed cells.[22]

We previously described the uncatalyzed 1,3-dipolar cycloaddition between phenyl azide **1a** and acrolein (Fig. 1a).[23] The reaction proceeds to give 4-formyl-1,2,3-triazoline **2a**, which immediately isomerized into the 4-formyl-2*H*-1,2,3-triazoline **3a** or oxidized into 4-formyl-1,2,3-triazole **4a**. The triazolines with electron-withdrawing substituents in the C4-position also undergo rearrangement to give the aliphatic α-diazocarbonyl compound **5a**.[24–28] The reaction of phenyl azide **1a**, under physiological conditions, is highly chemoselective to acrolein. We utilized the TAMRA-labeled phenyl azide, namely click-to-sense (CTS) probe **1b** (Fig. 1b(i)), for acrolein detection in cells undergoing oxidative stress and found that the CTS probe **1b** could shuttle in and out of cells through transporter-mediated mechanisms (ESI, Fig. S2a†).[29] If the CTS probe **1b** encounters the endogenous intracellular acrolein, the 1,3-dipolar cycloaddition occurs to produce a triazoline compound, rearranges into a diazo derivative, and reacts with the nearest organelle to anchor the fluorophore *via* covalent attachment.

We found that the CTS probe **1b** could be used selectively and sensitively to detect acrolein in live cells by observing the fluorescence intensity (Fig. 1b(i)). We demonstrated the feasibility of the method to determine acrolein levels in various human cell lines. In general, we found that cancer cells have a high level of acrolein, approximately between 50–250 nM, whereas healthy cells contain a negligible amount of acrolein (Fig. 1b(ii)).[30] In other words, endogenous cellular acrolein could be used as a new cancer marker. Furthermore, we utilized CTS probe **1b** to detect acrolein in breast cancer tissues resected from patients with breast cancer (ESI, Fig. S2b†).[30] This method selectively labels the cellular contents of cancer cells within live tissues and visualizes their morphology. The CTS probe **1b** has clinical significance in evaluating cancer morphology, and this method has been used in a clinical study as a highly selective,

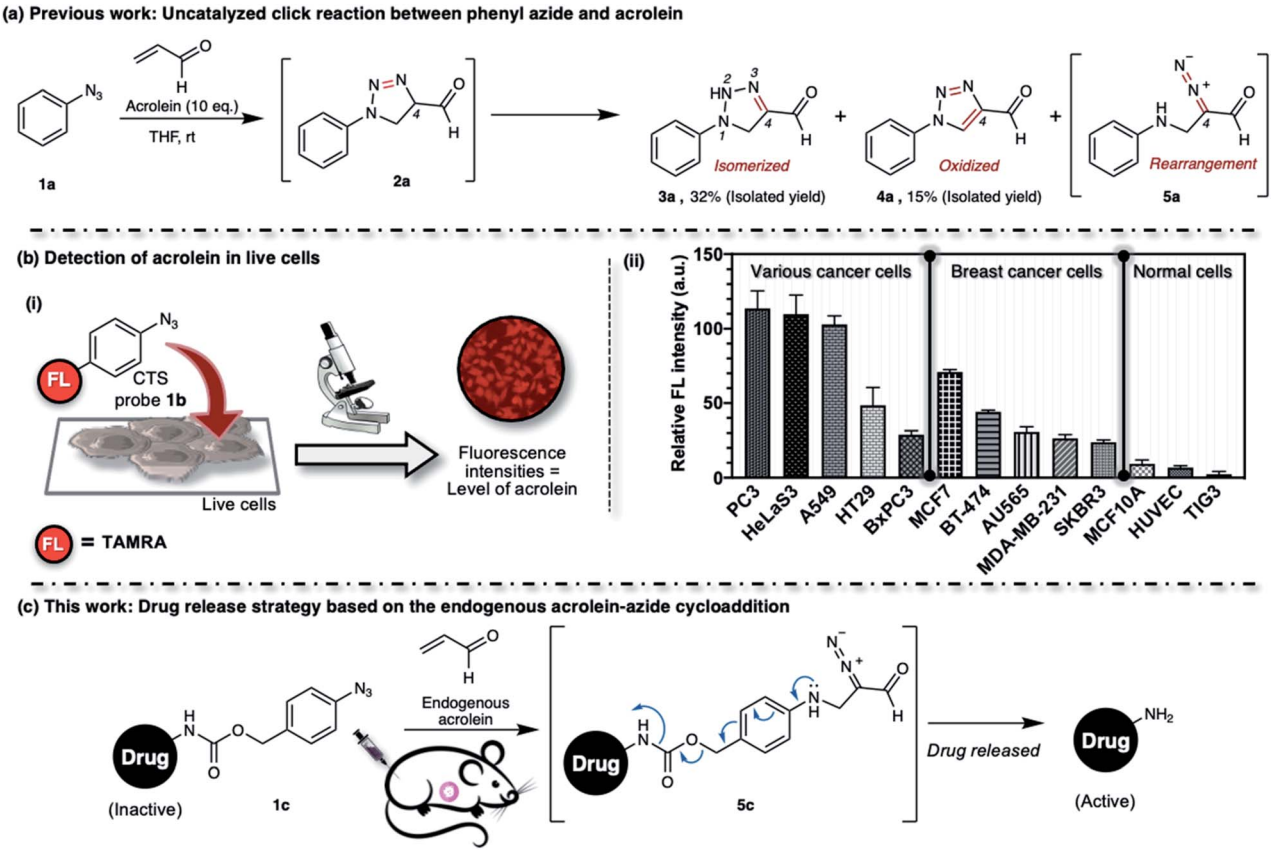

Fig. 1 (a) Phenyl azide **1a** reacts with acrolein through 1,3-dipolar cycloaddition to give intermediate **2a**, which could isomerize, oxidize, or rearrange to **3a**, **4a**, or **5a**, respectively. (b(i)) CTS probe **1b** selectively reacts with intracellular acrolein. (b(ii)) Fluorescence intensity, which was proportional to the intracellular acrolein concentration, was observed for each cell line over the CTS probe **1b** (22.5 μM). Various human cancer cell lines: PC3 (prostate cancer cell), HeLaS3 (cervical cancer cell), A549 (lung cancer cell), HT29 (colon cancer cell), BxPC3 (pancreatic cancer cell). Human breast cancer cell lines: MCF7 ($ER^+/PR^+/HER2^-$), BT-474 ($ER^+/PR^+/HER2^+$), AU565 ($ER^-/PR^-/HER2^+$), MDA-MB-231 ($ER^-/PR^-/HER2^-$), SKBR3 ($ER^-/PR^-/HER2^+$). Human normal cell lines: MCF-10A (mammary cell), HUVEC (umbilical vein endothelial cell), TIG3 (diploid cell). Immunoprofiles of the breast cancer subtypes are shown in the brackets; ER = estrogen receptor; PR = progesterone receptor; HER2 = human epidermal growth factor receptor-2. TAMRA = 5(6)-carboxytetramethylrhodamine. (c) Our *in vivo* drug release strategy utilizes the 1,3-dipolar cycloaddition between aryl azide and endogenous acrolein.

low-cost, and easy-to-perform method for cancer screening during breast cancer surgery.[31] Considering all of the above, we aim to develop an aryl azide–acrolein reaction-based prodrug, which could be applied to most cancer types. We recognized that if a benzyl carbamate linker is attached to the phenyl azide at a *para*-position, such as in compound **1c** (Fig. 1c), the reaction with endogenous acrolein will give the diazo compound **5c**, which could have potential in cancer-targeted prodrug activation strategies. If it succeeds, this method eliminates the need for pretreatments to accumulate exogenous enzymes or other activating agents on the cancerous tissues before prodrug administration, making it more realistic for practical application.

Results and discussion

Thus far, azide is known to be one of the most effective and widely used bioorthogonal reagents.[32] It was believed that azide is inert and will not react with any endogenous molecules in biosystems. Despite these assumptions, we found that aryl azide (CTS probe **1b**, Fig. 1b(i)) could react with endogenous acrolein generated by cancer cells in the absence of a catalyst.[23,29,30] Although the simple phenyl azide, such as in CTS probe **1b**, is convenient for the azide–acrolein 1,3-dipolar cycloaddition, as demonstrated herein for the drug release application, we thought that a high reactive aryl azide derivative would be more suitable to ensure efficient payload release at a low concentration within a reasonable timescale.

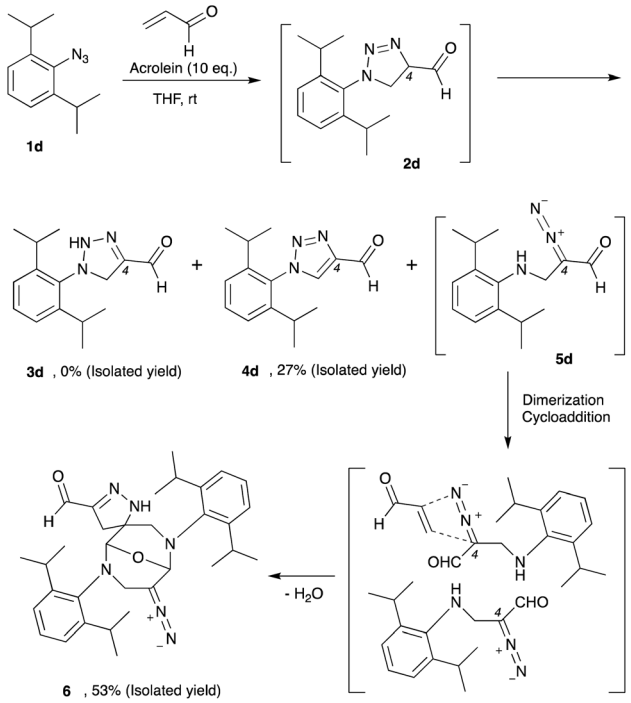

Fig. 2 The 2,6-diisopropylphenyl azide **1d** reacts with acrolein through 1,3-dipolar cycloaddition to give intermediate **2d**, which could isomerize, oxidize, or rearrange to **3d**, **4d**, or **5d**, respectively. The α-diazocarbonyl **5d** was isolated as heterocycle **6**.

Previously, Hosoya and co-workers reported that the 2,6-diisopropylphenyl azide **1d** (Fig. 2), despite its steric hindrance, reacts significantly faster than phenyl azide **1a** in the 1,3-dipolar cycloaddition with an alkyne.[33] While the azide–alkyne cycloaddition proceeds in a concerted manner,[34,35] it is more likely that the azide–acrolein cycloaddition proceeds in a stepwise manner. Therefore, we thought it was necessary to analyze the reactivity of phenyl azide **1a** and 2,6-diisopropylphenyl azide **1d** toward acrolein. First, the acrolein–phenyl azide **1a** (Fig. 1a and ESI, Fig. S3†) and the acrolein–2,6-diisopropylphenyl azide **1d** (Fig. 2 and ESI, Fig. S4†) reactions were analyzed by reversed phased high-performance liquid chromatography (RP-HPLC). The results showed that, while phenyl azide **1a** reacts with acrolein to give 4-formyl-2*H*-1,2,3-triazoline **3a** and 4-formyl-1,2,3-triazole **4a**, in the case of 2,6-diisopropylphenyl azide **1d**, the possible product 4-formyl-2*H*-1,2,3-triazoline **3d** could not be isolated from the reaction mixture (Fig. 2 and ESI, Fig. S4†). On the other hand, the reaction proceeds to give 4-formyl-1,2,3-triazole **4d** and α-diazocarbonyl compound **5d**, isolated as heterocycle **6** in good yields. It is reasonable to assume that diazo **5d** reacts further through dimerization, cycloaddition with one more acrolein molecule, and intramolecular acetal formation to give the heterocycle **6**.

We then design an experiment to determine the reaction kinetics for these acrolein–azide 1,3-dipolar cycloadditions (ESI, Fig. S5†). Since the triazoline **2a** and **2d** are difficult to observe due to the rapid isomerization, oxidation, or rearrangement of the intermediates to the corresponding products, we then performed the quantitative analysis by observing the formation of compound **3a**, **4d**, and **6**. We found that the second-order rate constant (k) for the reaction of 2,6-diisopropylphenyl azide **1d** with acrolein to give heterocycle **6** ($k = 3.8 \times 10^{-1}$ M^{-1} min^{-1}) was 9.7 times higher than the reaction of phenyl azide **1a** with acrolein to give triazoline **3a** ($k = 3.9 \times 10^{-2}$ M^{-1} min^{-1}). Also, we observed that in the reaction of 2,6-diisopropylphenyl azide **1d** and acrolein, the formation of heterocycle **6** was 6.6 times faster than the formation of 4-formyl-1,2,3-triazole **4d** ($k = 5.7 \times 10^{-2}$ M^{-1} min^{-1}).

Furthermore, we monitored the reaction of a 1 : 1 mixture of **1a** and **1d** with an excess amount of acrolein in $CDCl_3$ by ^{1}H-NMR spectroscopy and observed that the cycloaddition products from **1d** predominate (ESI, Fig. S6†). In contrast, the cycloaddition products from **1a** are hardly observed in the reaction mixture. Therefore, these results also demonstrate that the 2,6-diisopropylphenyl azide **1d** reacts more quickly than phenyl azide **1a** toward acrolein.

To rationalize the enhanced reactivity of 2,6-diisopropyl derivatives, we performed a density functional theory (DFT) calculation to determine the cyclization's reaction barrier (Fig. 3). The activation energy of the 2,6-diisopropylphenyl azide **1d**–acrolein cycloaddition (reaction 2) was lower than that of the phenyl azide **1a**–acrolein cycloaddition (reaction 1) by 6.2 kJ mol^{-1} (Fig. 3a). We carried out a distortion/interaction analysis[36] and a noncovalent interaction (NCI) analysis[37] to uncover the activation energy difference. Fig. 3b shows that the smaller distortion energy and the larger interaction energy magnitude causes the lower activation energy in reaction 2. The

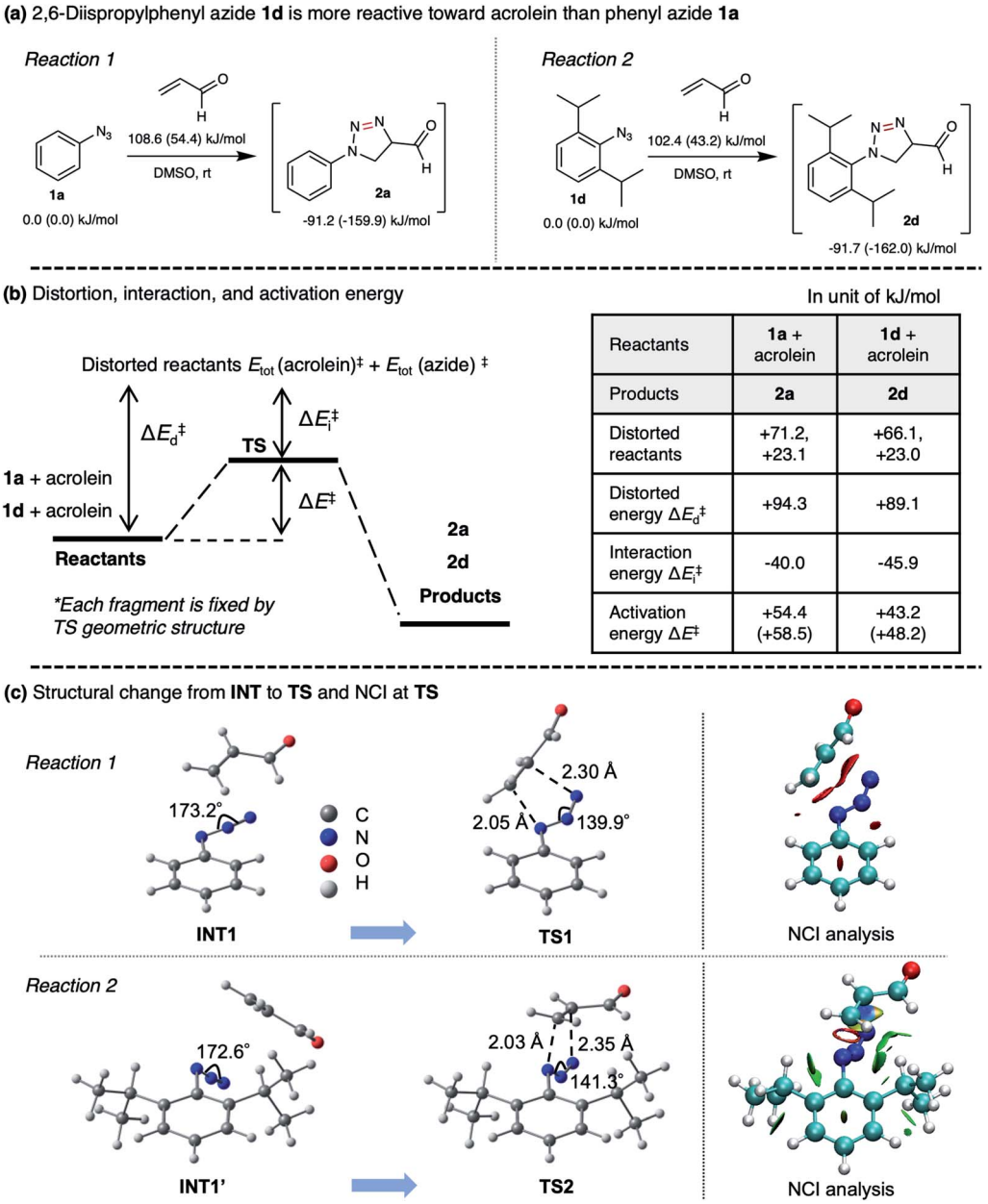

Reactants	1a + acrolein	1d + acrolein
Products	**2a**	**2d**
Distorted reactants	+71.2, +23.1	+66.1, +23.0
Distorted energy ΔE_d‡	+94.3	+89.1
Interaction energy ΔE_i‡	-40.0	-45.9
Activation energy ΔE‡	+54.4 (+58.5)	+43.2 (+48.2)

Fig. 3 (a) Calculated activation energies and reaction energies in reactions 1 and 2 at the ωB97XD/D95V(d) level combined with the SMD solvation model (DMSO). Values outside and inside parentheses correspond to Gibbs energy at room temperature and electronic energy, respectively. (b) Results of the distortion/interaction analysis which decomposes the activation energy (ΔE) into distortion (ΔE_d) and interaction (ΔE_i) energies. (c) Structural changes from pre-reaction intermediate (INT) to transition state (TS) in the cyclization step and noncovalent interaction (NCI) at TS visualized by the NCI analysis. NCI depicted in red and green corresponds to steric repulsion and week van der Waals (vdW) attraction.

smaller distortion energy in reaction 2 can be explained by the smaller structural change from INT1′ to TS2, as depicted in Fig. 3c. This substituent effect would be caused by the steric hindrance of the isopropyl groups, as discussed for the 1,3-dipolar cycloaddition of **1d** with diyne.[33] The NCI visualized in Fig. 3c demonstrates a weak attraction around the isopropyl groups in TS2, explaining the larger interaction energy magnitude in reaction 2. Therefore, compared to **1a**, the reactivity of **1d** with acrolein is enhanced by the isopropyl groups. The calculation result also explains that the regioselectivity of **2d** over **2d′** (ESI, Fig. S7†) is induced by the kinetic advantage of the reaction between *s-trans*-acrolein and the 2,6-diisopropylphenyl azide major conformer. The DFT calculation result is in good agreement with the experimental observation.

The production of heterocycle **6** and hence the presence of diazo **5d** in the reaction mixture, and the higher reactivity of 2,6-diisopropylphenyl azide **1d** toward acrolein encourages us to test the azide–acrolein cycloaddition for our drug release

strategy. As proof of concept, we designed coumarin-azidobenzylcarbamate (ABC) **7** (Fig. 4a). If successful, upon reaction with acrolein, the coumarin moiety will be released, producing an increase in fluorescence intensity that could be easily detected (ESI, Fig. S8a†). The synthesis started from 2,6-diisopropyl aniline, which was iodinated at the *para*-position to give 4-iodo-2,6-diisopropyl aniline **S1** in 98% yield (Fig. 4b). Palladium-catalyzed carbonylation allows the introduction of the ester group to afford compound **S2** in an 86% yield. An attempt to reduce the ester with $LiAlH_4$ gave the desired alcohol **S3** only in low yield while the undesired 4-methyl-2,6-diisopropyl aniline was obtained as the main product. We overcame this problem by utilizing DIBAL-H to smoothly reduce the ester to alcohol **S3** in 99% yield. The amino moiety of compound **S3** was then converted to an azide moiety using $NaNO_2$ and NaN_3 to give compound **S4** in an 85% yield. The reaction of compound **S4** with 7-amino-4-methylcoumarin in the presence of triphosgene and Hünig's base affords the desired coumarin-ABC **7** in 84% yield.

The coumarin-ABC **7** has good solubility in PBS with 1% DMSO (ESI, Fig. S8c†); also, the azide moiety is stable and not easily reduced under physiological conditions or by endogenous reductants, such as glutathione (GSH), in live cells. We examined the stability of coumarin-ABC **7** (20 μM) by incubating with GSH (20 μM in DMSO or 2 mM in PBS) and monitored the released coumarin by RP-HPLC analysis (Fig. 5a(i) and ESI, Fig. S8e(i)†). The result shows that even after 12 hours of incubation, the azide moiety was not susceptible to reduction, and the coumarin was not released as confirmed by RP-HPLC analysis. On the other hand, when coumarin-ABC **7** (20 μM) was incubated with acrolein (20 μM) in DMSO, the amount of released coumarin increases as the reaction time increases (Fig. 5a(ii)). We also examine the coumarin release kinetics and found that the second-order rate constant (k) was 5.1×10^{-2} mM^{-1} min^{-1} (ESI, Fig. S9†). A quantitative analysis estimated

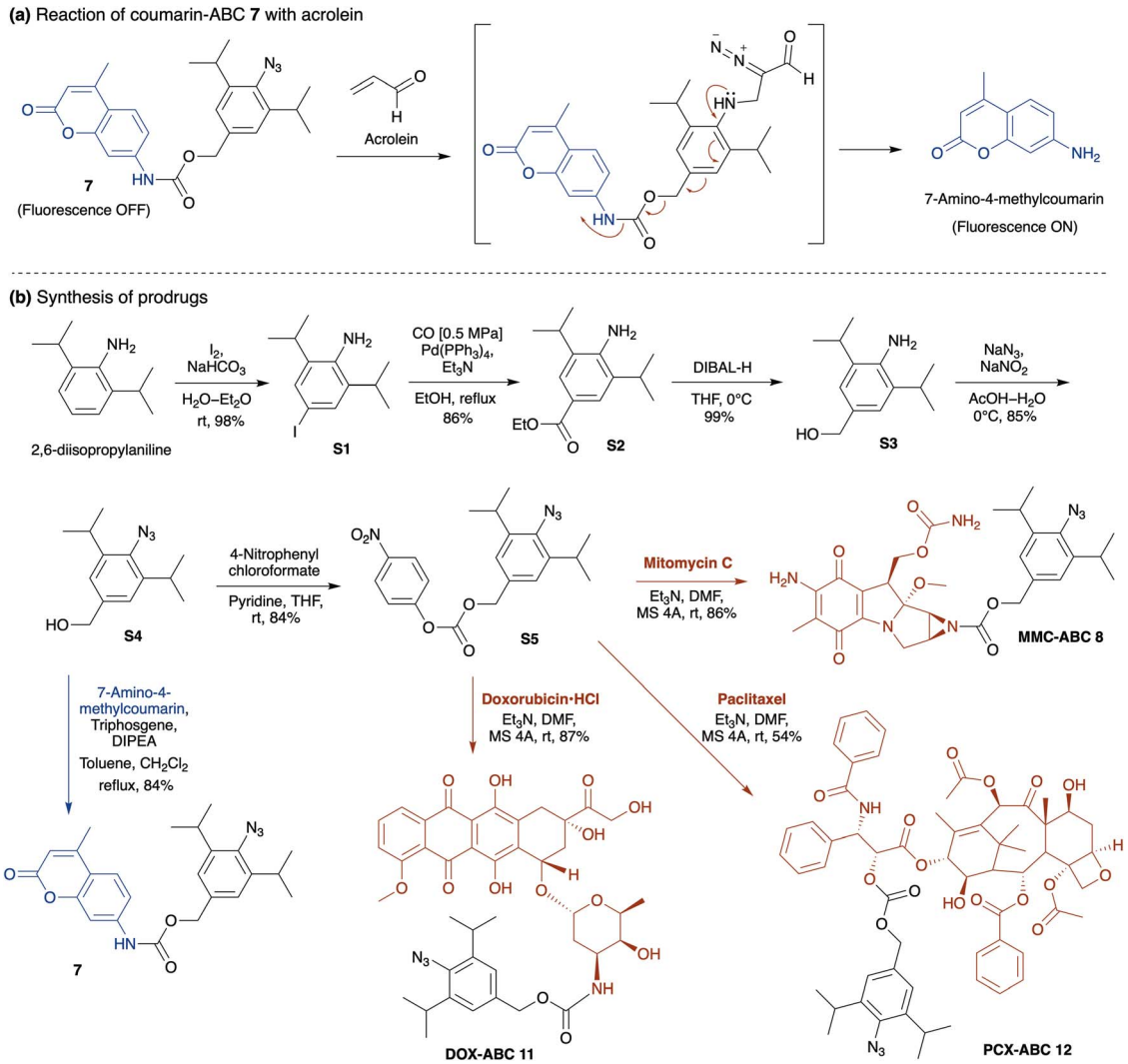

Fig. 4 (a) The reaction of coumarin-ABC **7** with acrolein to give α-diazocarbonyl compound induces the coumarin release. (b) The coumarin-ABC **7** could be synthesized from 2,6-diisopropylaniline. The reaction of compound **S4** with 4-nitrophenyl chloroformate proceeds to give intermediate **S5**, which could easily transform to prodrug MMC-ABC **8**, DOX-ABC **11**, and PCX-ABC **12**.

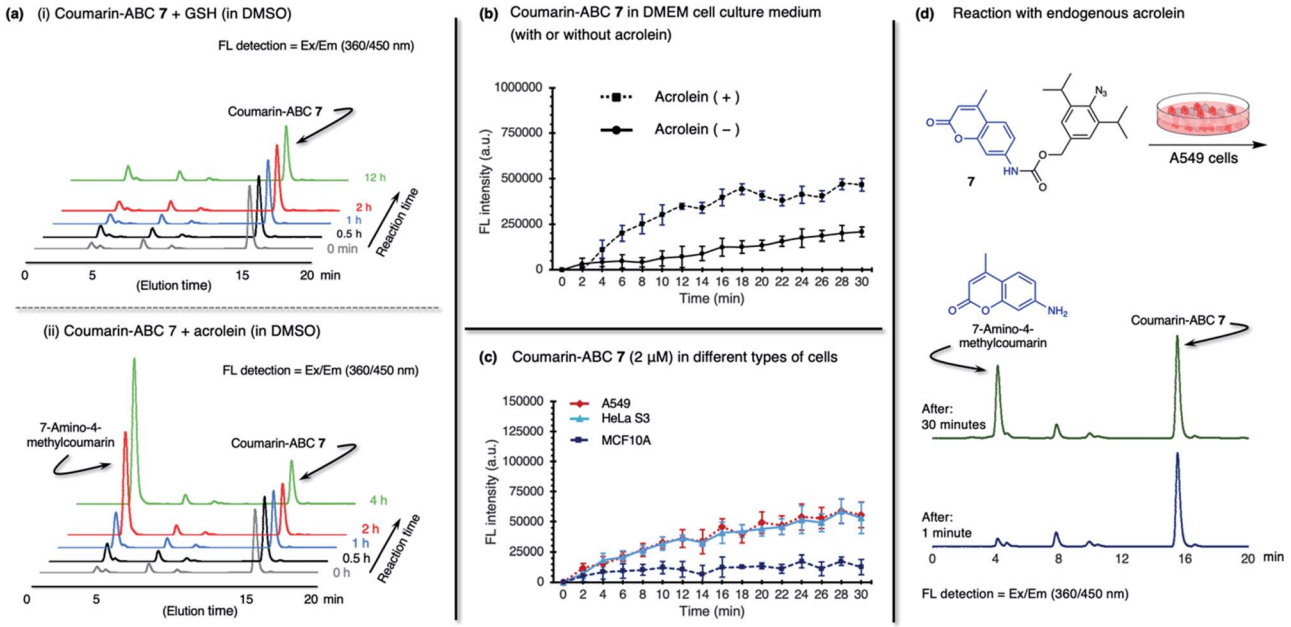

Fig. 5 The reactions between coumarin-ABC 7 (1.0 eq.) and (a(i)) glutathione (GSH, 1.0 eq.), or (a(ii)) acrolein (1.0 eq.) in DMSO were monitored at a specific time, by directly injecting the reaction mixtures to HPLC. (b) The coumarin-ABC 7 (20 μM) is incubated in Dulbecco's Modified Eagle's Medium (DMEM) solution with the presence (dashed line) or absence (solid line) of acrolein at room temperature. (c) Two cancer cells (A549, HeLa S3); and one normal cell (MCF10A) were treated with 2 μM of coumarin-ABC 7. Fluorescence intensity was normalized for each cell line per 10 000 cells. (d) The coumarin-ABC 7 (20 μM) was incubated in A549 cells. We used HPLC to analyze the cell culture medium at 1 min and 30 min of incubation.

that approximately 16 μM of coumarin was released from 150 μM of coumarin-ABC 7 after 4 hours of incubation with acrolein (ESI, Fig. S12†). Furthermore, we incubated coumarin-ABC 7 (20 μM) in Dulbecco's Modified Eagle's Medium (DMEM) solution with or without acrolein at room temperature (Fig. 5b). In the presence of acrolein, the coumarin-ABC 7 reacts with acrolein to give a diazo derivative that could induce coumarin release and translate into fluorescence activation. In the absence of acrolein, we observed a slight increase of fluorescence signal, probably due to carbamate hydrolysis in DMEM solution. Nevertheless, the carbamate hydrolysis in DMEM solution proceeds slower than the coumarin release triggered by the azide–acrolein reaction.

Based on the fact that acrolein is overproduced in cancer,[30] we then incubated coumarin-ABC 7 in two types of cancer cells. Herein, we decided to utilize A549 (human lung cancer) and HeLa S3 (human cervical cancer) cells because they have a relatively higher acrolein level than other cancer cells, as shown in Fig. 1c(ii). We also used a normal cell, MCF10A (normal human mammary cells), as control cells that produce a negligible amount of acrolein. The acrolein generated by cancer cells might remain inside the cell membrane or excrete outside the cells,[38] in this case to the culture medium. Therefore, in this *in vitro* cell experiment, we targeted both the intracellular and extracellular acrolein to react with coumarin-ABC 7. We treated the cells with coumarin-ABC 7 and directly observed the fluorescence change of cells in a culture medium every 2 minutes for 30 minutes. Incubation of 2 μM of coumarin-ABC 7 in cancer cells could initiate the reaction with the acrolein and trigger the coumarin release, as indicated by the increase in fluorescence intensity (Fig. 5c). On the contrary, the increase in fluorescence intensity in coumarin-ABC 7 treated normal cells was not significant. Following this procedure, A549 cells, HeLa S3 cells, and MCF10A cells were treated with coumarin-ABC 7 in five different concentrations in the presence or absence of 1 mM of *N*-acetyl cysteine (NAc-Cys), an acrolein scavenger, at room temperature for 60 minutes (ESI, Fig. S10†). The total fluorescence intensity of the cells was recorded using a spectrofluorometer. We observed decreased fluorescence intensity from the cells pretreated with NAc-Cys, indicating a lower amount of endogenous acrolein that could trigger the released coumarin.

We also confirmed the *in vitro* azide–endogenous acrolein 1,3-dipolar cycloaddition by observing the coumarin molecule's release with RP-HPLC analysis (Fig. 5d). We treated A549 cells with 20 μM of coumarin-ABC 7 and analyzed its HPLC profile at 1 minute and 30 minutes after incubation. As a result, the released 7-amino-4-methyl coumarin peak appeared in the analysis of the cell culture 30 minutes after incubation. Hence, these results prove that coumarin-ABC 7 selectively reacts with the endogenous acrolein produced by cancer cells. Also, we examined the stability of coumarin-ABC 7 in mouse blood serum and mouse liver microsome and found the half-life was 23.5 min and 22.8 min, respectively (ESI, Fig. S8e(ii) and (iii)†).

Taking into account the above results, for the *in vivo* cancer treatment study, we decided to replace the coumarin moiety with anticancer drugs, *i.e.*, mitomycin C (MMC),[39] doxorubicin (DOX),[40] and paclitaxel (PCX)[41] (Fig. 4b). MMC is an antibiotic

that was initially approved as a cancer chemotherapeutic agent in 1974 by the Food and Drug Administration (FDA). MMC with an alkyl group on the aziridine ring's nitrogen atom is known to have lower cytotoxicity than free MMC.[42–44] The mechanism of action of MMC is based on reductive activation and alkylation of DNA forming DNA adducts.[45] Unlike many other chemotherapy agents, MMC is usually not associated with multidrug resistance. However, its problematic safety profile, mainly due to its sub-acute and cumulative toxicity to bone marrow and kidney, is a significant obstacle to exploiting its substantial tumors activity.[42]

On the other hand, although DOX has been reported to be effective against breast, lung, and ovarian cancers,[46] it could also induce cardiotoxicity.[47,48] DOX acts on cancer cells through two possible mechanisms: (i) intercalation into DNA and disruption of topoisomerase-II-mediated DNA repair, or (ii) generation of free radicals and their damage to DNA, proteins, and cellular membranes.[49] Meanwhile, PCX, a microtubule-stabilizing drug used to treat ovarian, breast, and lung cancer, is recognized to induce mitotic arrest that leads to cell death in a subset of the affected population.[50,51] Our prodrugs can be prepared by reacting intermediate compound **S4** with 4-nitrophenyl chloroformate to give the activated carbonate **S5** in 84% yield (Fig. 4b). Then, the ester–amide exchange reaction of **S5** with the MMC, DOX, and PCX gives the desired prodrug MMC-ABC **8**, DOX-ABC **11**, and PCX-ABC **12** in 86%, 87%, and 54% yields, respectively.

In the *in vitro* cytotoxic assay, the free MMC and DOX nonspecifically showed cytotoxicity toward normal and cancer cells (Table 1 and ESI, Fig. S11a and b†). However, in MMC-ABC **8** or DOX-ABC **11**, it showed good selectivity against cancer cell lines. Against MCF10A cells, both MMC-ABC **8** and DOX-ABC **11** displayed low cytotoxicity. On the other hand, when cancer cells (*i.e.*, A549, HeLa S3) were treated with MMC-ABC **8** or DOX-ABC **11**, the endogenous acrolein overexpressed in the cancer cells reacted with the azide moiety of MMC-ABC **8** or DOX-ABC **11** to induce the release of payload drugs. The cytotoxicity of prodrug MMC-ABC **8** and DOX-ABC **11** in these cancer cells increased substantially. Notably, in the case of MMC-ABC **8**, it approached the cytotoxic level of free MMC. Nonetheless, the *in vitro* cytotoxic assay of PCX-ABC **12** showed cytotoxicity against the normal MCF10A cells (ESI, Fig. S11c†). The toxic nature of PCX and the drug-carbonate linkage with different properties with drug-carbamate linkage is not suitable for our strategy. Therefore, we excluded PCX-ABC **12** for further study.

Because MMC-ABC **8** has better drug release efficacy compared to DOX-ABC **11** to give selective cytotoxicity at a similar level as that of the free MMC, we decided to focus on prodrug MMC-ABC **8** for further investigation. When cancer cells were pretreated with NAc-Cys, the endogenous acrolein was scavenged; thus, treatment with MMC-ABC **8** showed no cytotoxicity against both A549 and HeLa S3 cells (Table 1 and ESI, Fig. S11a†). This result proved that MMC-ABC **8** reacts with endogenous acrolein produced by cancer cells to release the payload drug and produce its cytotoxic effect. As another control experiment, we also treated both normal and cancerous cells with 4-methyl-2,6-diisopropyl-phenyl azide **9** (chemical structure shown in Fig. 6a) and found that its cytotoxicity was negligible. In other words, without linkage to drugs, the aryl azide or the reaction of aryl azide with acrolein itself does not induce any cytotoxicity. Furthermore, through quantitative analysis, we found that incubation of MMC-ABC **8** (150 μM) with acrolein for 4 hours released approximately 18 μM of MMC, whereas in the case of DOX-ABC **11** (150 μM), approximately 13 μM of DOX was released (ESI, Fig. S12†).

To assess whether the strategy would work *in vivo* and result in the intended anticancer effect, we tested our prodrug system in living mice. For our first trial of *in vivo* study, we prepared A549 cell xenograft-bearing nude mice model. Our previous study estimated that approximately 200 nM of acrolein could be generated by A549 cells (2.5×10^5 cells per mL). However, before performing *in vivo* experiments, it was crucial to examine the acrolein levels in cancer tissues implanted into nude mice. The CTS probe **1b** (Fig. 1b and ESI, Fig. S2†) has been utilized to differentiate cancer and normal tissues from tumor stumps resected from patients with breast cancer with high selectivity and sensitivity. We considered that CTS probe **1b** might help determine the level of acrolein in the cancerous tissue surface of the mice. We therefore excised the mouse skin around the cancerous area to expose the tumor, including the border of cancerous and healthy tissue (area 1) and the healthy tissue (area 2) (ESI, Fig. S13†). The CTS probe **1b** (20 μM) was sprayed carefully on the surface area, and the whole mouse body was directly analyzed by fluorescence imaging. We found that the tumor area's fluorescence intensity is higher than area 1 and area 2, which proved that acrolein is overproduced by the mouse xenograft model's cancer tissue.

Table 1 IC_{50} values[a] for drugs and prodrugs determined in the MCF10A, A549 and HeLaS3 cells using the ATP assay

Compound	MCF10A (IC_{50}, μM)	A549 (IC_{50}, μM)	HeLaS3 (IC_{50}, μM)
MMC-ABC **8**	—[b]	2.707 (1.929–3.798)	0.671 (0.591–0.761)
MMC	0.724 (0.437–1.200)	0.901 (0.739–1.098)	0.332 (0.273–0.405)
NAc-Cys + **8**	—[b]	9.966 (7.934–12.52)	6.069 (5.499–6.697)
Compound **9**	—[b]	13.07 (7.780–21.95)	13.11 (9.755–17.61)
DOX-ABC **11**	—[b]	1.226 (0.979–1.535)	0.858 (0.811–0.908)
DOX	0.014 (0.002–0.135)	0.194 (0.161–0.233)	0.273 (0.167–0.446)

[a] 95% confidence interval ($n > 5$) is shown in the brackets. [b] No reduction in proliferation observed compared to untreated control.

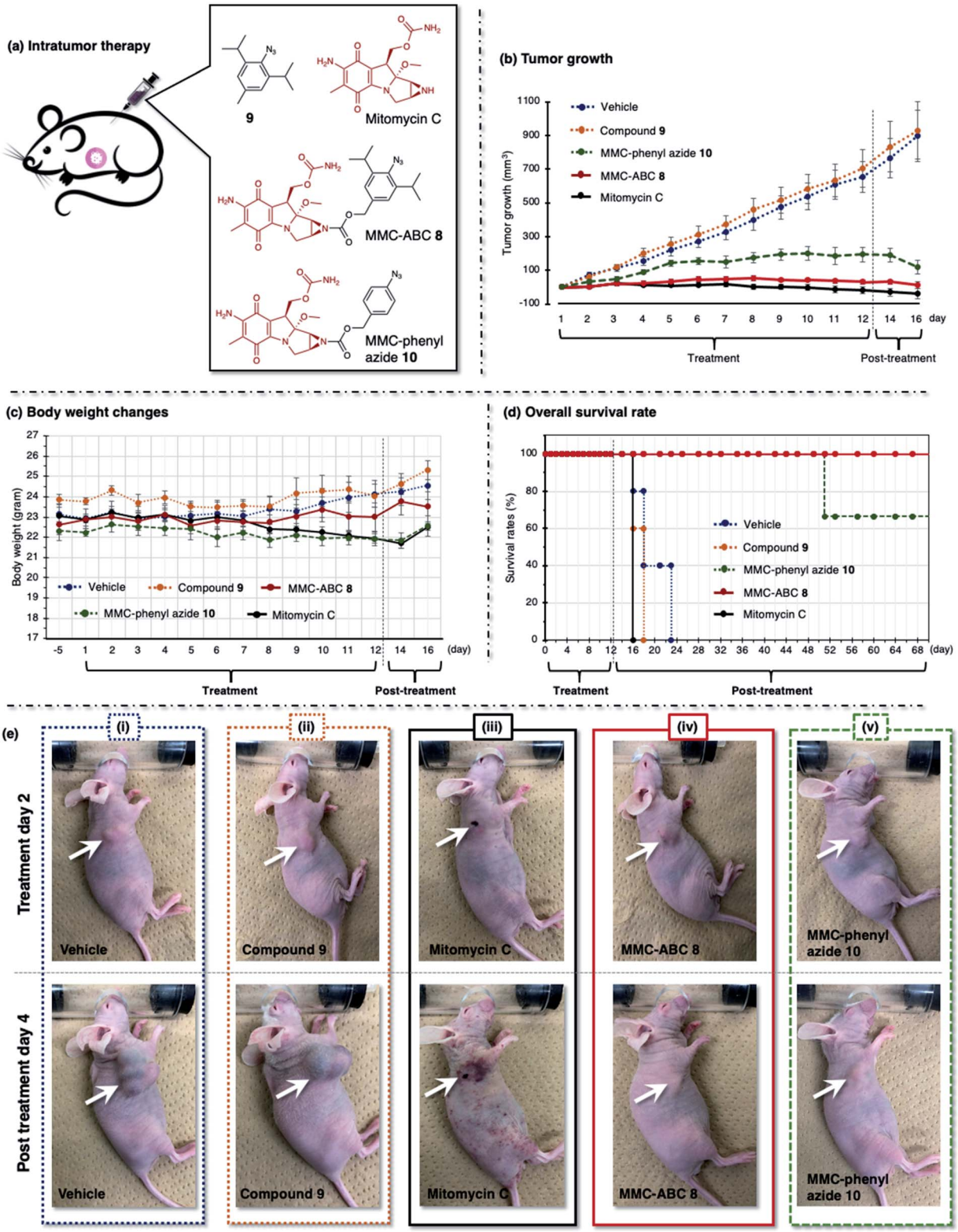

Fig. 6 (a) The A549 cell xenograft-bearing nude mice were treated with vehicle, prodrug MMC-ABC **8**, compound **9**, MMC-phenyl azide **10**, and free MMC. The compounds were administered intratumorally every day for 12 days, and the (b) tumor growth levels, (c) body weight changes, and (d) survival rates were observed. (e) The photos were taken during the second day of treatment and the fourth day after treatment. The arrow shows the location of cancer. See ESI Fig. S14 and S15† for other photos.

Based on the standard fluorescence intensity, approximately 10 μM of acrolein is generated on the mouse xenograft model's cancer tissue (1 × 1 cm). The amount is much higher than the acrolein generated by the A549 cell culture. Accordingly, we predicted that the *in vivo* endogenous acrolein–azide cycloadditions that trigger drug release would proceed more efficiently than *in vitro* cell experiments.

Therefore, we decided to intratumorally (Fig. 6) and intravenously (Fig. 7) treat a group of A549 cell xenograft-bearing nude mice with prodrug MMC-ABC **8** and compared them with other groups treated with vehicle, compound **9**, MMC-phenyl azide **10**, and free MMC. The MMC-phenyl azide **10** is derived from phenyl azide **1a** and has lower reactivity toward acrolein (*vide supra*), and hence is expected to have a decreased ability to release the drug (see ESI† for MMC-phenyl azide **10** preparation). The appropriate dose of mitomycin C for mouse experiments has been reported previously, with the maximum non-lethal dose being 6.7 mg kg^{-1} and the rational dose being 1.7 mg kg^{-1} (120 nmol).[52]

First, we treated the cancer-bearing xenograft mouse with a repeated intratumoral injection every day for 12 days and observed tumor growth (Fig. 6 and ESI, Fig. S14 and S15†). We found that treatment with vehicle (DMSO : EtOH : saline = 1 : 4 : 5, 5 μL, $n = 6$) or compound **9** (5 μL, 120 nmol, 1.2 mg kg^{-1}, $n = 6$) does not retard the tumor growth, and we observed a robust increase in tumor size (900 mm^3) in two weeks (Fig. 6b, dashed blue and orange line). As a result, these groups survived less than twelve days after treatment (Fig. 6d, dashed blue and orange line). Meanwhile, treatment with free MMC (5 μL, 120 nmol, 1.8 mg kg^{-1}, $n = 6$) significantly inhibits tumor growth (Fig. 6b, solid black line). However, despite its ability to inhibit tumor growth, this group survived less than five days after treatment (Fig. 6d, solid black line). The survival rate was even lower than that of the groups treated with vehicle and compound **9**. This result might be caused by the ADR effect of free MMC on the mouse, as we observed that the mouse had more body weight loss (Fig. 6c, solid black line) and inflammation on the whole body (Fig. 6e(iii), photo of post-treatment day 4).

We found that cancer treatment was effective on the mouse subjected to prodrug MMC-ABC **8** (5 μL, 120 nmol, 3.2 mg kg^{-1}, $n = 6$) (Fig. 6b, solid red line). Furthermore, we did not observe tumor regrowth even after the end of the treatment (ESI, Fig. S15b†). The average body weight could be maintained throughout the experiment (Fig. 6c, solid red line), and this group could survive up to two months after the treatment finished (Fig. 6d, solid red line). Inflammation and ADRs did not occur (Fig. 6e(iv), photo of post-treatment day 4), which proved that the prodrug specifically activated only at the desired cancer area and that cancer treatment with MMC-ABC **8** is promising. On the other hand, treatment with MMC-phenyl azide **10** (5 μL, 120 nmol, 2.8 mg kg^{-1}, $n = 6$) could inhibit the tumor growth to some extent (Fig. 6b, dashed green line). Even though the survival rate (Fig. 6d, dashed green line) is higher than the control experiment, it is still lower than the group treated with MMC-ABC **8**. We consider that this result is caused by the low reactivity of the MMC-phenyl azide **10** toward acrolein.

Alternatively, we treated the cancer-bearing xenograft mouse with a repeated intravenous injection every three days for ten days (four times injection) and observed tumor growth (Fig. 7 and ESI, Fig. S16–S21†). The drug concentration of the intravenous injection was two times higher than that of the intratumor injection. Herein, we could observe a similar tendency, as we observed from the intratumoral injection. We found that treatment with vehicle (DMSO : EtOH : saline = 1 : 4 : 5, 100 μL, $n = 8$) or compound **9** (100 μL, 240 nmol, 2.2 mg kg^{-1}, $n = 8$) does not have any effect, as the tumor growth was not retarded, and we observed an increase of tumor size (800 mm^3) by two weeks (Fig. 7b, dashed blue and orange line). As a result, these groups survived less than three weeks after treatment (Fig. 7d, dashed blue and orange line). Meanwhile, both prodrug MMC-ABC **8** (100 μL, 240 nmol, 6.2 mg kg^{-1}, $n = 8$) (Fig. 7b, solid red line) and MMC-phenyl azide **10** (100 μL, 240 nmol, 5.2 mg kg^{-1}, $n = 8$) (Fig. 7b, dashed green line) could inhibit the tumor growth, but the tumor inhibitory efficacy was more significant for prodrug MMC-ABC **8**. We found that the group treated with prodrug MMC-ABC **8** (Fig. 7d, solid red line) has a higher survival rate than the group treated with MMC-phenyl azide **10** (Fig. 7d, dashed green line). The treatment of the mice with free MMC (100 μL, 240 nmol, 3.6 mg kg^{-1}, $n = 8$) also significantly inhibited tumor growth (Fig. 7b, solid black line). Nevertheless, the body weight loss was very drastic (Fig. 7c, solid black line). If we compare the photos between the first day and the tenth day of treatment with MMC (Fig. 7e(iii)), we could notice the body size difference and inflammation in the tail area (ESI, Fig. S18†). Hence, the group treated with free MMC could not survive before the fourth injection (Fig. 7d, solid black line). Furthermore, to demonstrate that the observed therapeutic effect of MMC-ABC **8** is indeed mediated by acrolein-induced release, we treated another cancer-bearing xenograft mouse with compound **9** (5 μL, 120 nmol, 1.2 mg kg^{-1}, $n = 8$) intratumorally to eliminate the endogenous acrolein before injecting MMC-ABC **8** (100 μL, 240 nmol, 6.2 mg kg^{-1}, $n = 8$) intravenously. As a result, in this compound **9** and MMC-ABC **8** co-treated mouse group, we observed that the tumor growth increased significantly as the control group (Fig. 7b, dashed grey line, and photos in ESI, Fig. S21†).

To make a rough prediction on the stability of the prodrug *in vivo*, we performed RP-HPLC analysis of tumor and urine extracts from the mice models, two hours after prodrug MMC-ABC **8** and free MMC were intratumorally administered (ESI, Fig. S22†). In mice treated with MMC-ABC **8**, we found that some prodrug was remaining on the tumor (Fig. S22b†), and almost no prodrug or released MMC was detected in urine (Fig. S22c†). Simultaneously, in mice treated with free MMC, the free drug could not be detected from the tumor (Fig. S22b†), but the secreted MMC drug was present in the urine (Fig. S22c†). This result suggests that MMC-ABC **8**, which stays for longer time in the cancerous tissue, might gradually release MMC and gives its cytotoxic effect only at the desired target area. Based on the equilibrium dialysis method, we found that serum protein binding notably increased by

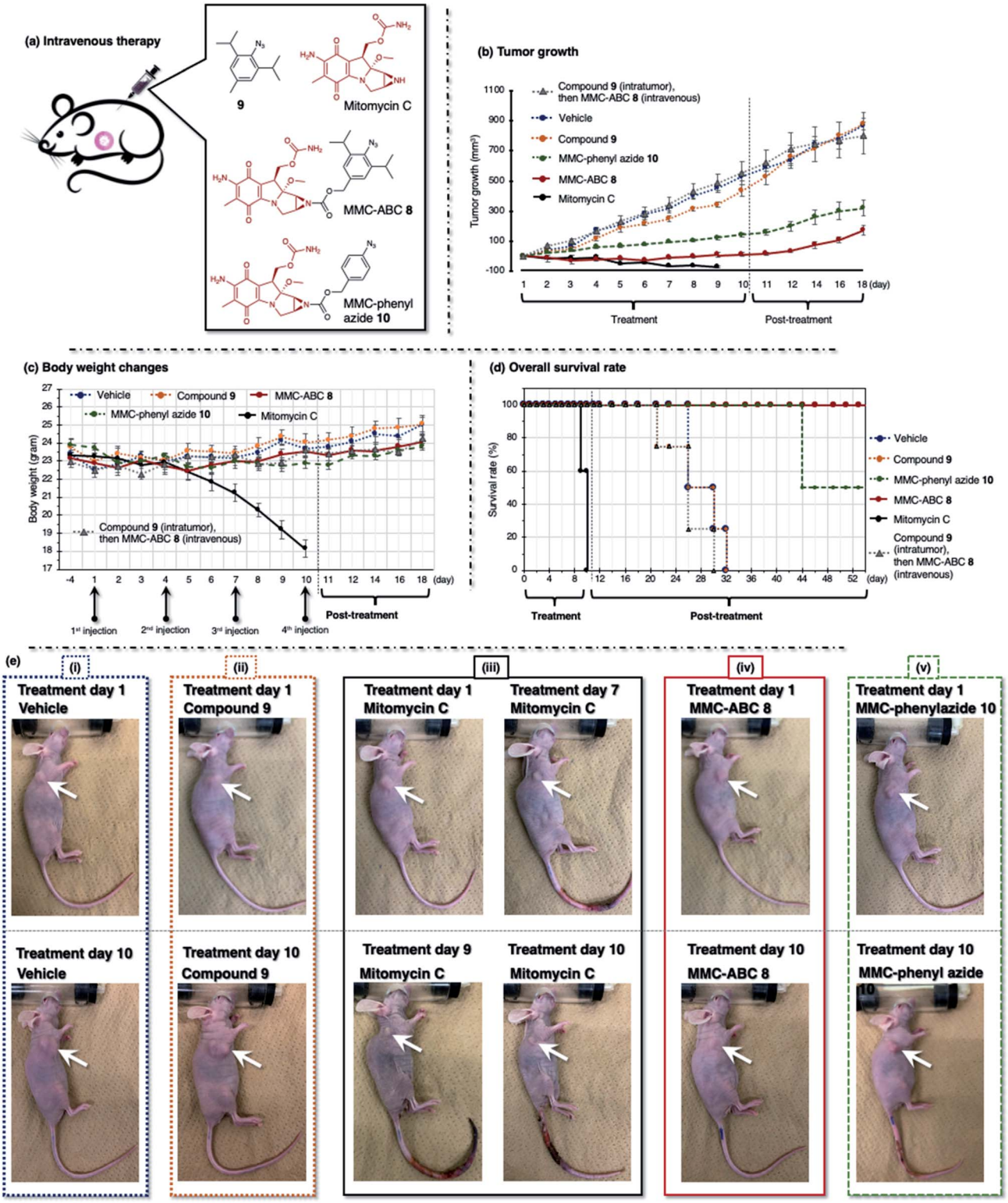

Fig. 7 (a) The A549 cell xenograft-bearing nude mice were treated with vehicle, prodrug MMC-ABC **8**, compound **9**, MMC-phenyl azide **10**, and free MMC. The compounds were administered intravenously every three days for ten days, and the (b) tumor growth levels, (c) body weight changes, and (d) survival rates were observed. (e) The photos were taken during the first and tenth day of treatment. The arrow shows the location of cancer. See ESI Fig. S16–S21† for other photos.

derivatizing the parent compounds to the ABC compounds (*e.g.*, 44% to >95% in the case of coumarin). Nevertheless, we also observed that the free ligands could be released upon treatment with acrolein (ESI, Fig. S8d†). Therefore, similar to the clinically used drugs (*e.g.*, vinblastine, warfarin)[53,54] with high serum binding affinity, we considered that the stabilized

ABC prodrugs–protein complex is efficiently carried to the cancer region and activated by acrolein.

Herein, we have described the stability and selectivity of prodrug MMC-ABC **8** and shown that intratumor and intravenous administration does not affect its efficacy. Moreover, since acrolein is generally overproduced by most cancer cells, we anticipate that our strategy might be useful for further applications in other different cancer types. In the literature (ESI, Fig. S1b and c†),[11,12] drug-conjugated phenyl azide, such as **1c** (Fig. 1c), did not show cytotoxicity *in vitro* experiments with cancer cells. Moreover, to trigger the drug release, it is typically co-treated with other activating agents, such as phosphine reagent.[11] Based on our results, the lower acrolein level in cancer cell cultures compared to living mice (*vide supra*) might affect the azide reaction toward endogenous acrolein. Also, we found that replacing the phenyl azide moiety with the more reactive 2,6-diisopropyl azide could increase its reaction kinetics toward endogenous acrolein in the mouse model's cancerous tissues, triggering the drug release.

Conclusions

In conclusion, we have developed a strategy for an *in vivo* anticancer drug delivery by utilizing endogenous acrolein–azide cycloaddition to trigger the drug release. This method enabled controlled prodrug activation by targeting cancer cells that produced a high acrolein level, including HeLa S3 and A549. The 2,6-diisopropylphenyl azide moiety of MMC-ABC **8** was efficiently reacted with endogenous acrolein to trigger drug release. The overall *in vitro* results showed a significant increase in the potency of prodrug **8** against cancerous tissues and satisfactory selectivity for cancerous over non-cancerous cells. Animal studies further validated our prodrug's excellent efficiency for *in vivo* tumor inhibition, as well as its biosafety. This method was applied to the A549 cancer-bearing xenograft mouse model, and it shows promising results, where cancer growth was inhibited, and the ADR effect was reduced. As shown in this study, the MMC-ABC **8** remains in cancer cells and the drug is released only at the desired target area. It is noteworthy that the dose applied in the current study was below the maximum tolerant dose of MMC. Furthermore, the ABC moiety could be easily conjugated with other types of drugs. Therefore, it could be applied to other cytotoxic drugs that cause a high rate of ADRs. In other words, this method may significantly expand the scope of anticancer therapeutic agents.

Author contributions

Conceptualization: A. R. P., and K. Tanaka; formal analysis: T. I., and S. M.; funding acquisition: A. R. P., and K. Tanaka; investigation: A. R. P., P. A., K. Terashima, K. M., M. F.; visualization: A. R. P.; writing-original draft preparation: A. R. P., and K. Tanaka; writing-review and editing: A. R. P., and K. Tanaka.

Conflicts of interest

There are no conflicts to declare.

Acknowledgements

All animal procedures were performed in accordance with the Guidelines for Care and Use of Laboratory Animals of RIKEN and approved by the Animal Ethics Committee of RIKEN (W2019-2-049). This work was financially supported by JSPS KAKENHI [Grant Numbers JP16H03287, JP18K19154, JP15H05843 (to K. Tanaka) and JP18K14341, JP18K07265, 18H05503 (to A. R. P.)]. Funding was also provided by the Russian Government Program for Competitive Growth (to Kazan Federal University). The authors are also grateful to Professor Takamitsu Hosoya and Associate Professor Suguru Yoshida of the Tokyo Medical and Dental University for their fruitful discussion on bulky aryl azide at the very beginning of this research.

References

1 K. Nurgali, R. T. Jagoe and R. Abalo, *Front. Pharmacol.*, 2018, **9**, 245.
2 S. K. Sharma and K. D. Bagshawe, *Adv. Drug Delivery Rev.*, 2017, **118**, 2–7.
3 Y. Wang, S. Song, J. Liu, D. Liu and H. Zhang, *Angew. Chem., Int. Ed.*, 2015, **54**, 536–540.
4 D. Neri and C. T. Supuran, *Nat. Rev. Drug Discovery*, 2011, **10**, 767–777.
5 I. A. Müller, F. Kratz, M. Jung and A. Warnecke, *Tetrahedron Lett.*, 2010, **51**, 4371–4374.
6 C. Li and S. Wallace, *Adv. Drug Delivery Rev.*, 2008, **60**, 886–898.
7 J. Khandare and T. Minko, *Prog. Polym. Sci.*, 2006, **31**, 359–397.
8 R. Duncan, *Nat. Rev. Cancer*, 2006, **6**, 688–701.
9 X. Ji, Z. Pan, B. Yu, L. K. De La Cruz, Y. Zheng, B. Ke and B. Wang, *Chem. Soc. Rev.*, 2019, **48**, 1077–1094.
10 M. Azoulay, G. Tuffin, W. Sallem and J.-C. Florent, *Bioorg. Med. Chem. Lett.*, 2006, **16**, 3147–3149.
11 R. van Brakel, R. C. M. Vulders, R. J. Bokdam, H. Grull and M. S. Robillard, *Bioconjugate Chem.*, 2008, **19**, 714–718.
12 S. S. Matikonda, D. L. Orsi, V. Staudacher, I. A. Jenkins, F. Fiedler, J. Chen and A. B. Gamble, *Chem. Sci.*, 2015, **6**, 1212–1218.
13 R. M. Versteegen, R. Rossin, W. ten Hoeve, H. M. Janssen and M. S. Robillard, *Angew. Chem., Int. Ed.*, 2013, **52**, 14112–14116.
14 E. M. Herrlinger, M. Hau, D. M. Redhaber, G. Greve, D. Willmann, S. Steimle, M. Muller, M. Lubbert, C. C. Miething, R. Schule and M. Jung, *ChemBioChem*, 2020, **21**, 2329–2347.
15 J. Rao, A. Dragulescu-Andrasi and H. Yao, *Curr. Opin. Biotechnol.*, 2007, **18**, 17–25.
16 Y. Zheng, X. Ji, B. Yu, K. Ji, D. Gallo, E. Csizmadia, M. Zhu, M. R. Choudhury, L. K. C. De La Cruz, V. Chittavong, Z. Pan, Z. Yuan, L. E. Otterbein and B. Wang, *Nat. Chem.*, 2018, **10**, 787–794.
17 J. P. Kehrer and S. S. Biswal, *Toxicol. Sci.*, 2000, **57**, 6–15.

18 K. Muguruma, A. R. Pradipta, Y. Ode, K. Terashima, H. Michiba, M. Fujii and K. Tanaka, *Bioorg. Med. Chem.*, 2020, **28**, 115831.
19 G. Houen, K. Bock and A. L. Jensen, *Acta Chem. Scand.*, 1994, **48**, 52–60.
20 R. A. Alarcon, *Arch. Biochem. Biophys.*, 1970, **137**, 365–372.
21 K. Uchida, *Trends Cardiovasc. Med.*, 1999, **9**, 109–113.
22 R. Shi, T. Rickett and W. Sun, *Mol. Nutr. Food Res.*, 2011, **55**, 1320–1331.
23 A. R. Pradipta, M. Taichi, I. Nakase, E. Saigitbatalova, A. Kurbangalieva, S. Kitazume, N. Taniguchi and K. Tanaka, *ACS Sens.*, 2016, **1**, 623–632.
24 C.-H. Yang, L.-T. Lee, J.-H. Yang, Y. Wang and G.-H. Lee, *Tetrahedron*, 1994, **50**, 12133–12142.
25 G. T. Anderson, J. R. Henry and S. M. Weinreb, *J. Org. Chem.*, 1991, **56**, 6946–6948.
26 W. Broeckx, N. Overbergh, C. Samyn, G. Smets and G. L'abbé, *Tetrahedron*, 1971, **27**, 3527–3534.
27 K. R. Henery-Logan and R. A. Clark, *Tetrahedron Lett.*, 1968, **9**, 801–806.
28 R. Huisgen, G. Szeimies and L. Möbius, *Chem. Ber.*, 1966, **99**, 475–490.
29 A. R. Pradipta, M. Fujii, T. Tanei, K. Morimoto, K. Shimazu, S. Noguchi and K. Tanaka, *Bioorg. Med. Chem.*, 2019, **27**, 2228–2234.
30 T. Tanei, A. R. Pradipta, K. Morimoto, M. Fujii, M. Arata, A. Ito, M. Yoshida, E. Saigitbatalova, A. Kurbangalieva, J.-I. Ikeda, E. Morii, S. Noguchi and K. Tanaka, *Adv. Sci.*, 2019, **6**, 1801479.
31 A. R. Pradipta, T. Tanei, K. Morimoto, K. Shimazu, S. Noguchi and K. Tanaka, *Adv. Sci.*, 2020, **7**, 1901519.
32 M. F. Debets, C. W. J. van der Doelen, F. P. J. T. Rutjes and F. L. van Delft, *ChemBioChem*, 2010, **11**, 1168–1184.
33 S. Yoshida, A. Shiraishi, K. Kanno, T. Matsushita, K. Johmoto, H. Uekusa and T. Hosoya, *Sci. Rep.*, 2011, **1**, 82.
34 D. H. Ess and K. N. Houk, *J. Am. Chem. Soc.*, 2008, **130**, 10187–10198.
35 K. N. Houk, J. Sims, C. R. Watts and L. J. Luskus, *J. Am. Chem. Soc.*, 1973, **95**, 7301–7315.
36 F. M. Bickelhaupt and K. N. Houk, *Angew. Chem., Int. Ed.*, 2017, **56**, 10070–10086.
37 R. Laplaza, F. Peccati, R. A. Boto, C. Quan, A. Carbone, J. P. Piquemal, Y. Maday and J. Contreras-García, *Wiley Interdiscip. Rev.: Comput. Mol. Sci.*, 2020, e1497.
38 J. F. Stevens and C. S. Maier, *Mol. Nutr. Food Res.*, 2008, **52**, 7–25.
39 S. T. Crooke and W. T. Bradner, *Cancer Treat. Rev.*, 1976, **3**, 121–139.
40 W. E. Derek, N. Rashmi, C. Simon, M.-B. Kyle, P. J. M. Jonathan and M. P. Amadeo, *Curr. Drug Metab.*, 2015, **16**, 412–426.
41 M. Skwarczynski, Y. Hayashi and Y. Kiso, *J. Med. Chem.*, 2006, **49**, 7253–7269.
42 Y. Amitay, H. Shmeeda, Y. Patil, J. Gorin, D. Tzemach, L. Mak, P. Ohana and A. Gabizon, *Pharm. Res.*, 2016, **33**, 686–700.
43 T. Sun, A. Morger, B. Castagner and J. C. Leroux, *Chem. Commun.*, 2015, **51**, 5721–5724.
44 P. D. Bass, D. A. Gubler, T. C. Judd and R. M. Williams, *Chem. Rev.*, 2013, **113**, 6816–6863.
45 M. He, P. J. Sheldon and D. H. Sherman, *Proc. Natl. Acad. Sci. U. S. A.*, 2001, **98**, 926.
46 C. F. Thorn, C. Oshiro, S. Marsh, T. Hernandez-Boussard, H. McLeod, T. E. Klein and R. B. Altman, *Pharmacogenet. Genomics*, 2011, **21**, 440–446.
47 C. Carvalho, R. X. Santos, S. Cardoso, S. Correia, P. J. Oliveira, M. S. Santos and P. I. Moreira, *Curr. Med. Chem.*, 2009, **16**, 3267–3285.
48 S. M. Swain, F. S. Whaley and M. S. Ewer, *Cancer*, 2003, **97**, 2869–2879.
49 D. A. Gewirtz, *Biochem. Pharmacol.*, 1999, **57**, 727–741.
50 B. A. Weaver, *Mol. Biol. Cell*, 2014, **25**, 2677–2681.
51 S. B. Horwitz, *Ann. Oncol.*, 1994, **5**, S3–S6.
52 M. Inaba, T. Kobayashi, T. Tashiro and Y. Sakurai, *Japanese Journal of Cancer Research GANN*, 1988, **79**, 509–516.
53 T. Bohnert and L.-S. Gan, *J. Pharm. Sci.*, 2013, **102**, 2953–2994.
54 I. Petitpas, A. A. Bhattacharya, S. Twine, M. East and S. Curry, *J. Biol. Chem.*, 2001, **276**, 22804–22809.